Electrically pumped quantum post vertical cavity surface emitting lasers

Hyochul Kim, Matthew T. Rakher, Dirk Bouwmeester, and Pierre M. Petroff

Citation: Appl. Phys. Lett. **94**, 131104 (2009); doi: 10.1063/1.3112578

View online: https://doi.org/10.1063/1.3112578

View Table of Contents: http://aip.scitation.org/toc/apl/94/13

Published by the American Institute of Physics

Electrically pumped quantum post vertical cavity surface emitting lasers

Hyochul Kim,[1,a)] Matthew T. Rakher,[1,b)] Dirk Bouwmeester,[1,2] and Pierre M. Petroff[3,4]
[1]*Department of Physics, University of California Santa Barbara, Santa Barbara, California 93106, USA*
[2]*Huygens Laboratory, Leiden University, P.O. Box 9504, 2300 RA Leiden, The Netherlands*
[3]*Department of Materials, University of California Santa Barbara, Santa Barbara, California 93106, USA*
[4]*Department of ECE, University of California Santa Barbara, Santa Barbara, California 93106, USA*

(Received 26 January 2009; accepted 12 March 2009; published online 1 April 2009)

We demonstrate low threshold electrically pumped lasing in oxide apertured vertical cavity surface emitting lasers with quantum posts (QPs) as the active medium. A lasing threshold current as low as 12 μA is achieved at 7 K and room temperature continuous wave lasing is also demonstrated in the cavities with quality factors of ~10 000. At low temperature, the QP devices show remarkably lower lasing current thresholds compared to equivalent quantum dot devices. © *2009 American Institute of Physics*. [DOI: 10.1063/1.3112578]

Quantum dot (QD) lasers[1,2] based on small mode volume microcavities have been attractive for their low lasing thresholds. Small mode volume microcavities enable low lasing threshold by limiting the number of optical modes and enhancing the spontaneous emission coupling factor (β).[1–5] Furthermore, QD lasers show low lasing thresholds due to high material gain and a deltalike density of states.[6] However, the small filling factor of QDs imposes the use of very high QD densities or multiple QD layers as a gain medium for practical laser applications. As an alternative gain medium, we introduce a quantum post[7] (QP), which is a self assembled, height controlled nanorod grown by molecular beam epitaxy. A QP shows sharp excitonic luminescence and single photon emission.[8] Similar nanostructures such as columnar-dots have shown high lasing performance due to their large carrier collection efficiency and enhanced optical quality.[9] We demonstrate low threshold lasing in oxide apertured micropillar cavities[10] with a single layer of QPs as the gain medium and compare their lasing threshold characteristics to those of QD lasers with the same cavity design.

A QP is grown by covering an InAs/GaAs seed QD with successive stacks of 7 ML of GaAs and 1 ML of InAs layer cycles. Interruptions between alternating GaAs and InAs layer deposition provide the time for the indium to diffuse to the seed QD position, and produce the coherently strained InGaAs/GaAs post.[7] Figures 1(a) and 1(b) show the device structure and a transmission electron microscopy (TEM) image of QPs and the surrounding quantum well (QW) matrix. The QP electronic structure was calculated[11] using an effective mass eight band $k\cdot p$ model that includes strain effects, dimensions and compositions of the QPs, and surrounding matrix. It shows that electrons are delocalized within the QP, while the holes remain localized at the top or bottom QDs which terminate the QP. Unlike the QD, which contains only one z (along the growth axis) confined and two or three laterally confined electron states, the QP, depending on its height, can contain several (two to three or more) z confined and laterally confined states.[7,11]

In the experiments presented here, 30 nm high QPs are used as the gain medium in an oxide apertured micropillar cavity. The cavity structure [Fig. 1(c)] consists of an n-doped GaAs substrate followed by an n-doped bottom distributed Bragg reflector (DBR), a $\lambda/2n$ GaAs cavity (190 nm thick), an AlGaAs tapered oxide aperture, and a p-doped top DBR. The bottom (top) DBR consists of 32 (23) pairs of $\lambda/4$ GaAs (74 nm thick) and $Al_{0.9}Ga_{0.1}As$ (83.4 nm thick) layers. The interfaces between GaAs and $Al_{0.9}Ga_{0.1}As$ are graded for the bottom DBR, and bandgap engineered for the top DBR to reduce the device resistance.[12] The 30 nm high QPs are grown within the GaAs cavity at the antinode of the cavity field. For comparison, samples with a single layer of QDs as the active gain medium are grown with the same structure as that of the QP devices. The cavity length and DBR layer thickness of the QD samples are adjusted accordingly to ensure a better spectral overlap between the cavity mode and the QD emission. The QD samples are grown under the same conditions as the QP samples and the partially covered island technique is used to blueshift the QD photoluminescence

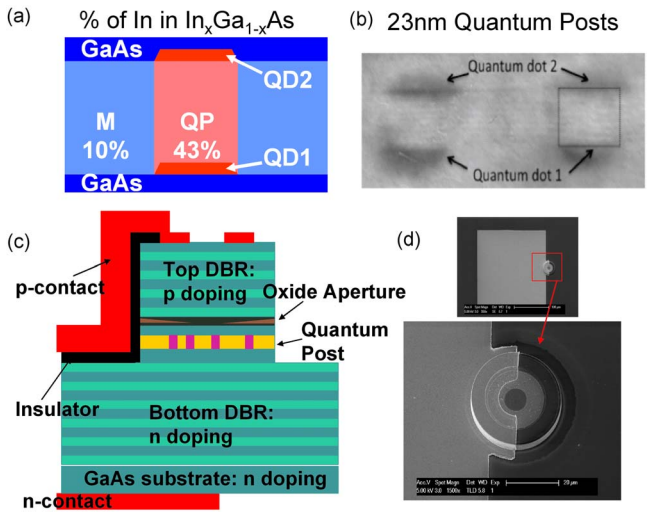

FIG. 1. (Color online) (a) Schematic of the QP structure and measured indium concentration in %. (b) Cross sectional TEM of two QPs. The two QDs at each ends of the QPs have an indium concentration of around 45%–48%. (c) Schematic view of a QP oxide apertured micropillar cavity laser. (d) SEM image after processing the ring and pad metal contacts.

[a)]Electronic mail: hckim@physics.ucsb.edu.
[b)]Present address: National Institute of Standards and Technology, Gaithersburg, Maryland 20899, USA.

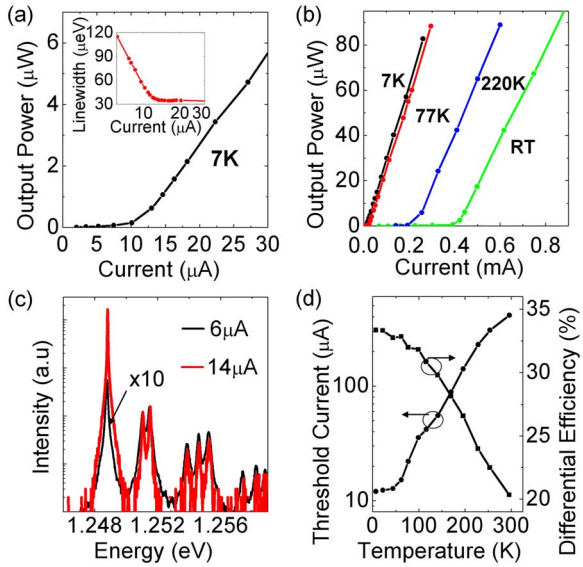

FIG. 2. (Color online) Characteristics of QP device with 3 μm diameter aperture. (a) *L-I* curve at 7 K. Threshold current is $I_{th} \simeq 12$ μA. The inset shows the linewidth of the fundamental cavity mode as a function of injection current. (b) *L-I* curves at various temperatures. (c) Lasing spectra in log scale at 7 K, $I=6$ μA (0.5 I_{th}, black), and 14 μA (1.2 I_{th}, red). (d) Lasing threshold current and differential quantum efficiency as a function of temperature.

(PL) wavelength.[7] The QD and QP density ($\sim 200/\mu m^2$) are identical in both types of devices.

To confine the mode laterally, 28 to 33 μm diameter pillars are etched by reactive ion etching using Cl_2, followed by an oxidation step[10] to make the oxide aperture which further confines the lateral mode to a few micrometers. Samples are mounted in a liquid helium flow cryostat with a temperature range adjustable from 4 K to room temperature (RT). For the PL and electroluminescence measurements, we collect the signal through a high magnification microscope objective, then send it to either a high resolution (~ 30 μeV) spectrometer with a liquid nitrogen cooled silicon charge coupled device or a power meter. All devices are investigated under continuous wave (CW) voltage bias condition.

We first investigate a QP device with a 3 μm diameter oxide aperture. As shown in Figs. 2(a) and 2(b), we observe a lasing threshold of 12 μA (~ 180 A/cm^2) at 7 K and 22 μA (~ 330 A/cm^2) at 77 K. Figure 2(c) shows a dominant peak associated with the fundamental cavity mode present at an injection current of 1.2 I_{th}. The second lasing mode does not appear below 1 mA injection current. This lasing threshold at 7 K is similar to the lasing threshold of QD laser with etched micropillar cavities.[2] The linewidth of the fundamental mode decreases with increasing injection current and saturates at ~ 35 μeV, limited by the spectrometer resolution [Fig. 2(a) inset]. The quality factor (Q) of the cavity mode is estimated as $\sim 10\,000$ below the lasing threshold. As shown in Fig. 2(d), the lasing threshold current increases from 12 μA at 7 K to 0.4 mA at RT, while the differential quantum efficiency decreases from 33% at 7 K to 20% at RT.

The lasing current threshold dependence on temperature for QP and QD devices turns out to be very different. Figures 3(a) and 3(b) show this dependence for QP and QD devices with aperture diameters of 2, 3, and 4 μm. To characterize

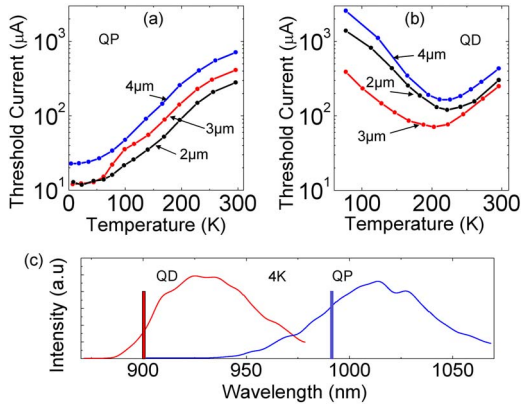

FIG. 3. (Color online) Comparison of the QD and QP device characteristics: lasing threshold currents as a function of temperature in (a) QP devices, (b) QD devices, (c) normalized QD (red) and QP (blue) PL spectra of calibration samples at 4 K pumped by a CW HeNe laser with 8 μW (350 W/cm^2) pump power. The cavity mode wavelengths of laser devices at 4 K are indicated with the red bar (QD devices) and blue bar (QP devices).

the wavelength and temperature dependence of the gain, PL measurements were performed on QD and QP calibration samples grown under the same conditions as the cavity samples [Fig. 3(c)]. The cavity modes of the QP and QD samples are blueshifted and detuned by ~ 45 meV from the ground state PL peak at 4 K. While QP devices show a minimum lasing threshold current at ~ 10 K, QD devices show a minimum lasing threshold current at ~ 220 K. This minimum for the QD devices is consistent with our PL measurement which shows the wetting layer frequency matching that of the lasing mode at this temperature. At 10 K, lasing is not observed below 1 mA injection current for the QD devices. Despite similar spectral overlap between the cavity mode and ground state emission and same densities ($\sim 200/\mu m^2$) of emitters, QP samples show about two orders of magnitude lower lasing thresholds than QD samples at ~ 10 K. We believe that the larger carrier capture cross sections and modal overlap[9] of QPs are one of the main reasons for their much lower lasing thresholds. The QP carrier collection efficiency can be also enhanced due to the surrounding QW matrix.[13] Another possible reason for the large threshold difference is the larger density of excited states of QPs than QDs.[7,11] For QD devices in this experiment, the modal gain from a single layer of QDs is saturated and this results in high lasing thresholds at low temperature. For QP devices, the additional density of excited states of QPs at the energy close to the lasing cavity modes can provide high saturation gain.[14,15]

Finally, Fig. 4 presents the intensity of the fundamental mode as a function of injection current for 2, 3, and 4 μm QP devices at 7 K. We calculate the spontaneous emission coupling factor β of these devices using the rate equation[16]

$$I(p) = A\left[\frac{p}{(1+p)}(1+\xi)(1+\beta p) - \xi\beta p\right], \quad (1)$$

where A is a scaling factor $A=\hbar\omega/\tau_{ph}\delta\beta$ and ξ is a dimensionless parameter $\xi=N_0\beta V\tau_{ph}/\tau_{sp}$. Here δ is the photon conversion efficiency, N_0 is the transparency carrier concentration, V is the active material volume, I is the injection current, and p is the photon number which is taken to be 1 at the lasing threshold. τ_{ph} is known from the cavity mode Q to be ~ 5 ps. N_0 is assumed to be 3×10^{17} cm^{-3} similar to the QD transparency carrier concentration.[17] The lateral filling

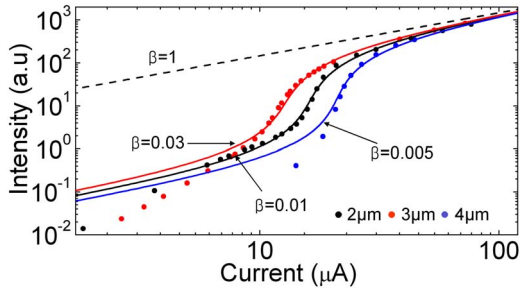

FIG. 4. (Color online) Log-log plot of the measured light intensity as a function of injection current for QP devices with 2 μm diameter (black data points), 3 μm diameter (red data points) and 4 μm diameter (blue data points) apertures. The fit curves are calculated with Eq. (1) for various numbers of β.

factor and τ_{sp} are assumed to be 0.2 and 150 ps for a 2 μm diameter device. We calculate a β of 0.01 for the 2 μm diameter device, 0.03 for the 3 μm diameter device, and 0.005 for the 4 μm diameter device. Additionally, β can be calculated from a simple mode counting argument,[18] and this yields a value of ~0.01 for the 2 μm diameter device, validating the aforementioned estimates. The *L-I* curves deviate from Eq. (1) at low injection currents, showing a superlinear behavior with slope of ~3 in a log-log plot. This deviation is related to the superlinear increase of PL intensity in the excited states and is less pronounced in smaller diameter devices where the number of QPs in the devices is reduced.

In conclusion, we have demonstrated electrically pumped CW lasing of QPs in oxide apertured micropillar cavities. With a cavity quality factor ~10 000, a lasing threshold current as low as 12 μA is achieved at 7 K. As an active gain medium, a single QP layer shows lasing with a current density below 200 A/cm^2 in a 3 μm diameter oxide apertured cavity. We attribute this low threshold to the enhanced carrier collection efficiency, large modal overlap, and the high saturation gain in the QPs.

This research has been supported by DARPA-ARL grant No. W911NF-07-1-0321. A portion of this work was done in the UCSB nanofabrication facility, part of the NSF funded NNIN network.

[1] S. Strauf, K. Hennessy, M. T. Rakher, Y. S. Choi, A. Badolato, L. C. Andreani, E. L. Hu, P. M. Petroff, and D. Bouwmeester, Phys. Rev. Lett. **96**, 127404 (2006).
[2] S. Reitzenstein, T. Heindel, C. Kistner, R. A. Iman, C. Schneider, S. Höfling, and A. Forchel, Appl. Phys. Lett. **93**, 061104 (2008).
[3] O. Painter, R. K. Lee, A. Scherer, A. Yariv, J. D. O'Brien, P. D. Dapkus, and I. Kim, Science **284**, 1819 (1999).
[4] H.-G. Park, S.-H. Kim, S.-H. Kwon, Y.-G. Ju, J.-K. Yang, J.-H. Baek, S.-B. Kim, and Y.-H. Lee, Science **305**, 1444 (2004).
[5] S. M. Ulrich, C. Gies, S. Ates, J. Wiersig, S. Reitzenstein, C. Hofmann, A. Löffler, A. Forchel, F. Jahnke, and P. Michler, Phys. Rev. Lett. **98**, 043906 (2007).
[6] M. Asada, Y. Miyamoto, and Y. Suematsu, IEEE J. Quantum Electron. **22**, 1915 (1986).
[7] J. He, H. J. Krenner, C. Pryor, J. P. Zhang, Y. Wu, D. G. Allen, C. M. Morris, M. S. Sherwin, and P. M. Petroff, Nano Lett. **7**, 802 (2007).
[8] H. J. Krenner, C. E. Pryor, J. He, and P. M. Petroff, Nano Lett. **8**, 1750 (2008).
[9] M. Sugawara, K. Mukai, Y. Nakata, K. Otsubo, and H. Ishilkawa, IEEE J. Sel. Top. Quantum Electron. **6**, 462 (2000).
[10] N. G. Stoltz, M. T. Rakher, S. Strauf, A. Badolato, D. D. Lofgreen, P. M. Petroff, L. A. Coldren, and D. Bouwmeester, Appl. Phys. Lett. **87**, 031105 (2005).
[11] H. J. Krenner, C. E. Pryor, J. He, J. P. Zhang, Y. Wu, C. M. Morris, M. Sherwin, and P. M. Petroff, Physica E (Amsterdam) **40**, 1785 (2008).
[12] C. W. Wilmsen, H. Temkin, and L. A. Coldren, *Vertical-Cavity Surface-Emitting Lasers: Design, Fabrication, Characterization, and Applications* (Cambridge University Press, London, 1999).
[13] G. T. Liu, A. Stintz, H. Li, T. C. Newell, A. L. Gray, P. M. Varangis, K. J. Malloy, and L. F. Lester, IEEE J. Quantum Electron. **36**, 1272 (2000).
[14] L. A. Coldren and S. W. Corzine, *Diode Lasers and Photonic Integrated Circuits* (Wiley, New York, 1995).
[15] G. Park, O. B. Shchekin, D. L. Huffaker, and D. G. Deppe, Appl. Phys. Lett. **73**, 3351 (1998).
[16] G. Björk and Y. Yamamoto, IEEE J. Quantum Electron. **27**, 2386 (1991).
[17] D. Englund, H. Altug, B. Ellis, and J. Vuckovic, Laser Photonics Rev. **2**, 264 (2008).
[18] If all modes have the same decay rate, β can be approximated as $(\lambda_0/n)^3\lambda_0/8\pi V_c\Delta\lambda$. λ_0 is a wavelength in free space, n is effective refractive index, V_c is cavity volume, and $\Delta\lambda$ is FWHM of the optical gain. With λ_0=990 nm, n=3.2, V_c=3 μm^3, and $\Delta\lambda$=40 nm, β of ~0.01 is obtained.